Zhang *et al.*
Chinese Journal of Mechanical Engineering (2024) 37:30
https://doi.org/10.1186/s10033-024-01006-8

Chinese Journal of Mechanical Engineering

ORIGINAL ARTICLE

Open Access

Experimental Study on Wire Melting Control Ability of Twin-Body Plasma Arc

Ruiying Zhang[1,2], Fan Jiang[3*] and Long Xue[1]

Abstract

The twin-body plasma arc has the decoupling control ability of heat transfer and mass transfer, which is beneficial to shape and property control in wire arc additive manufacturing. In this paper, with the wire feeding speed as a characteristic quantity, the wire melting control ability of twin-body plasma arc was studied by adjusting the current separation ratio (under the condition of a constant total current), the wire current/main current and the position of the wire in the arc axial direction. The results showed that under the premise that the total current remains unchanged (100 A), as the current separation ratio increased, the middle and minimum melting amounts increased approximately synchronously under the effect of anode effect power, the first melting mass range remained constant; the maximum melting amount increased twice as fast as the middle melting amount under the effect of the wire feeding speed, and the second melting mass range was expanded. When the wire current increased, the anode effect power and the plasma arc power were both factors causing the increase in the wire melting amount; however, when the main current increased, the plasma arc power was the only factor causing the increase in the wire melting amount. The average wire melting increment caused by the anode effect power was approximately 2.7 times that caused by the plasma arc power. The minimum melting amount was not affected by the wire-torch distance under any current separation ratio tested. When the current separation ratio increased and reached a threshold, the middle melting amount remained constant with increasing wire-torch distance. When the current separation ratio continued to increase and reached the next threshold, the maximum melting amount remained constant with the increasing wire-torch distance. The effect of the wire-torch distance on the wire melting amount reduced with the increase in the current separation ratio. Through this study, the decoupling mechanism and ability of this innovative arc heat source is more clearly.

Keywords Twin-body plasma arc, Melting control ability, Melting amount, Current separation ratio

1 Introduction

Wire arc additive manufacturing (WAAM) has become a cost-effective additive manufacturing method for metal components and can challenge traditional manufacturing technologies due to its advantages in manufacturing cost, material utilization and environmental dependence [1–3]. Most WAAM methods are developed based on traditional arc welding processes, such as plasma arc [4], gas tungsten arc [5, 6], variable polarity gas tungsten arc [7], ultrasonic frequency pulsed arc [8] and cold metal transfer process [9, 10]. The alternating current time cycle on layer height in WAAM based on a gas tungsten arc have been studied by Ayarkwa et al. [11]. Kazanas et al. [12] demonstrated that walls with various angles ranging from vertical to horizontal and closed shapes could be fabricated by WAAM based on cold metal transfer (CMT). Wang et al. [13] confirmed that the deposition

*Correspondence:
Fan Jiang
jiangfan@bjut.edu.cn
[1] School of Mechanical Engineering, Beijing Institute of Petrochemical Technology, Beijing 102617, China
[2] Beijing Academy of Safety Engineering and Technology, Beijing 102617, China
[3] College of Mechanical and Energy Engineering, Beijing University of Technology, Beijing 100124, China

rate increased linearly with the increasing wire size under the same heat input, and the bead geometry had a higher aspect ratio when the wire size was smaller in plasma arc additive manufacturing. Wang et al. [14] proposed twin-wire plasma arc additive manufacturing (PAAM), and the feasibility was verified. To further improve the efficiency and performance of WAAM, bypass coupling arc heat sources have been proposed and used in WAAM by researchers [15–17]. As the typical form of bypass coupling arc heat source, the arcing-wire gas tungsten arc is formed by adding a wire into the gas tungsten arc, and a side arc is established between the wire and tungsten, which establishes the gas tungsten arc (main arc) with the workpiece. A part of the total current that flows through the tungsten is separated from the main arc and flows into the wire. Thus, the melting amount of the wire (mass transfer) is not only dependent on the main arc and can be controlled effectively with the help of the wire current.

As an extension of the gas tungsten arc, the plasma arc has the advantages of excellent direction control and higher energy density. Zhang et al. [18] have proposed an arcing-wire plasma arc heat source based on the arcing-wire gas tungsten arc. An increasing number of studies have focused on WAAM development based on arcing-wire plasma arcs, which have been named double-electrode micro-plasma arc, bypass-current wire-heating plasma arc and twin-body plasma arc in different studies, they are collectively referred to as the twin-body plasma arc. Huang et al. [19] and Yu et al. [20] studied the dynamic behaviour of molten pools and microstructure and properties of formed parts in the additive manufacturing of twin-body plasma arc welding (TPAW). It was reported that with the increase in bypass current, the liquid metal flow in the molten pool became unstable, the dendrite arm spacing of the stacking sample first decreased and then increased, and the dendrite arm spacing of the stacking sample first increased and then decreased. Miao et al. [21] carried out research on droplet transfer behaviour in TPAW and reported that the droplet transfer form could be controlled accurately by using the coordinated control of the main/bypass current and other parameters. Zhang et al. [18] adopted two kinds of bypass power supply (a constant current power supply and a constant voltage power supply) to study the arc stability in TPAW and indicated that the arc stability is superior with this power supply than with other power supplies, as the bypass power supply is a constant current power supply. Zhang et al. [22] analysed the heat transfer mechanisms of wire in TPAW and showed that the total power transferred to the filler wire included the anode effect power and plasma arc power, which could increase significantly with increasing wire current. Zhang et al. [23] analysed the droplet transfer behaviour and the forces acting on the droplet in this process and reported that as the total current remained unchanged, the droplet transfer mode could be changed from globular to spray under the coordinated control of parameters, and spray transfer could be realized under a low current.

Previous studies [22, 23] have mainly carried out qualitative analysis on twin-body plasma arc, focusing on the droplet transfer behaviour, the heat transfer behaviour, and other properties of the formed part. However, exactly how this novel arc heat source decouples the mass and heat transfer is still not entirely understood. In this paper, the wire feeding speed is set as the characteristic quantity and used to calculate the melting amount of wire. The wire melting control ability of the twin-body plasma arc is studied under the condition of constant total current (total output) by changing the current separation ratio. Furthermore, the effect of the interaction between the wire current and main current on the wire melting increment is analysed by adjusting the wire current or main current. The effect of the position of the wire in the arc axial direction on melting amount of wire is studied by adjusting the distance between the filler wire and PAW torch (wire-torch distance) under different current separation ratios. The decoupling mechanism and ability of this innovative arc heat source will be more clear after this study.

2 Experimental Procedure

The twin-body plasma arc experimental system is shown in Figure 1. It includes a plasma arc welding (PAW) power supply, constant current power supply, PAW torch, gas metal arc welding (GMAW) torch, and workpiece, etc. The positive terminal of the PAW power supply is connected with the workpiece, and the negative terminal is connected with the PAW torch to form the main arc. The positive terminal of the constant current power supply is connected with the GMAW torch, and the negative terminal is also connected with the PAW torch to form the bypass arc. The total current (I) includes the main current (I_1) and wire current (I_2). The current separation ratio (CSR) is defined as the ratio of wire current (I_2) to total current (I). The signal acquisition system mainly includes a high-speed camera, current sensor, voltage sensor, and synchronization controller, etc. The high-speed camera is installed about 500 mm perpendicular to the plane determined by the PAW torch and GMAW torch, operating at 10000 Hz and 512×512 dpi. The arc images, current and voltage signals are detected, collected and recorded synchronously in the experimental process.

In the previous study, Zhang et al. [23] investigated the heat transfer mechanism of wire in twin-body

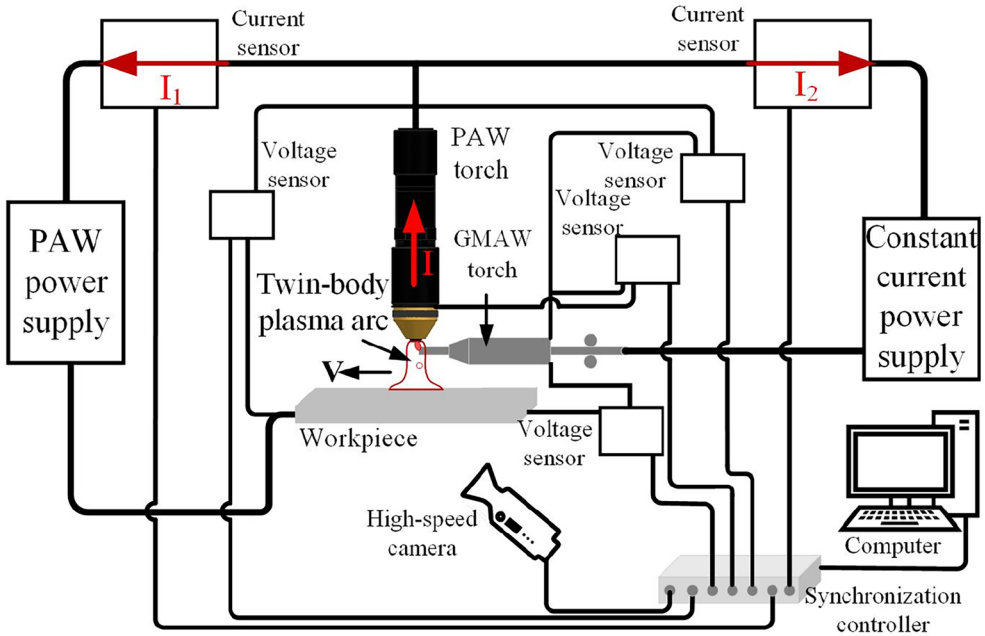

Figure 1 Schematic diagram of twin-body plasma arc

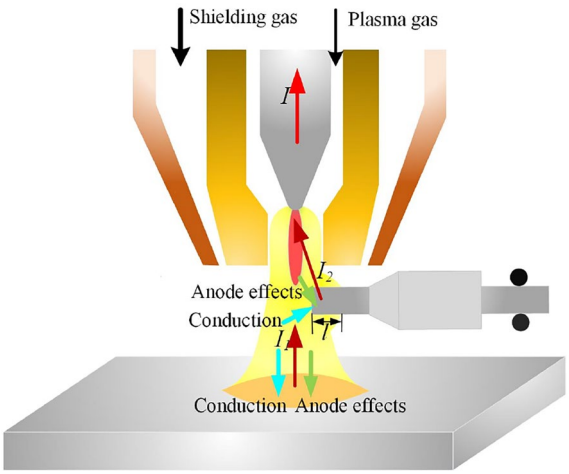

Figure 2 Heat transfer mechanism of wire in twin-body plasma arc

plasma arc. The total power transferred to the wire mainly comes from the plasma arc power and anode effect power due to the wire current, as shown in Figure 2. The plasma arc power acting on the wire is the power transferred to the wire from the plasma arc through thermal conduction. The anode effect power acting on the wire consists of the anode fall energy, electron thermal energy and condensation energy (work function) of the electrons.

The plasma arc power (Q_1) can be expressed as:

$$Q_1 \propto \lambda_g \left(\frac{\mathrm{d}(\lambda_g T)}{\mathrm{d}x_0} + 2\sum_1^n \frac{1}{n} \frac{\mathrm{d}(\lambda_g T)}{\mathrm{d}x_n} \right), \tag{1}$$

where λ_g is the thermal conductivity of the arc, $\mathrm{d}(\lambda_g T)/\mathrm{d}x$ is the temperature gradient in the arc near the anode, l is the wire length entering the plasma arc, n stands for the value that the filler wire is divided into several segments.

The anode effect power (Q_2) can be expressed as:

$$Q_2 = I_2 U_a + \frac{I_2}{e} \cdot \frac{3}{2} K (T_e - T_a) + I_2 \psi_a, \tag{2}$$

where I_2 is the wire current, U_a is the anode fall voltage, K is the Boltzmann's constant, T_e is the electron temperature, T_a is the electron temperature at the anode, ψ_a is the work function of the metal.

The total power acting on the wire (Q) can be expressed as:

$$Q = Q_1 + Q_2. \tag{3}$$

According to Eq. (1), the plasma arc power (Q_1) acting on the wire is controlled by the energy distribution of the plasma arc and l. When the total current and other related parameters for the plasma arc environment remain constant, the energy distribution of the plasma arc remains unchanged. Thus, the plasma arc power

is only determined by l, which is affected by the wire feeding speed. According to Eq. (2), the anode effect power (Q_2) acting on the wire is proportional to the wire current. Therefore, the influences of the current separation ratio, wire current/main current ratio, and position of the wire in the arc axial direction on the wire melting control ability are studied here.

To explore the wire melting control ability under the condition of a constant total current in the twin-body plasma arc, the minimum wire feeding speed, middle wire feeding speed and maximum wire feeding speed were selected as characteristic quantities, and the corresponding melting amount of the wire was calculated. The minimum wire feeding speed is the critical speed at which the wire melts at the arc edge on the feeding side, at which point a large droplet can be formed stably, although the bypass arc shows an unstable trend (as shown in Figure 3(a)). The middle wire feeding speed is that the wire melts at the central axis of the arc, where the stabilization of metal transfer is most easily realized (as shown in Figure 3(b)). The maximum wire feeding speed is the critical speed at which the wire melts at the arc edge, and the wire will directly pass through the arc without melting if the wire feeding speed is further increased (as shown in Figure 3(c)). The melting mass range is also set as a characteristic quantity, which is the difference in the melting amount corresponding to two different wire feeding speeds, to represent the control ability of wire melting in this heat source. The effects of current separation ratios of 0% (traditional plasma arc), 10% (wire current is 10 A), 30%, 50% and 70% on the control ability of wire melting are investigated on the premise of a total current of 100 A and the wire feed direction is nearly perpendicular to the direction of the PAW torch.

To explore the effect of the interaction between the wire current and main current on the wire melting increment, two methods were adopted. In the first method, the wire feeding speed is fixed, and the wire melting position in the arc radius direction is set as the characteristic quantity. In the second method, the wire melting position is fixed, and the wire feeding speed is set as the characteristic quantity. The study was carried out by increasing the wire current from 30 A to 100 A at an interval of 10 A while the main current remains at 50 A and by increasing the main current from 30 A to 100 A at an interval of 10 A while the wire current remains at 50 A.

The position of the wire in the arc axial direction is also an important factor affecting its melting amount. The changes in the position of the wire in the arc axial direction would change the plasma arc power, and then the total energy acting on the wire changes. The position

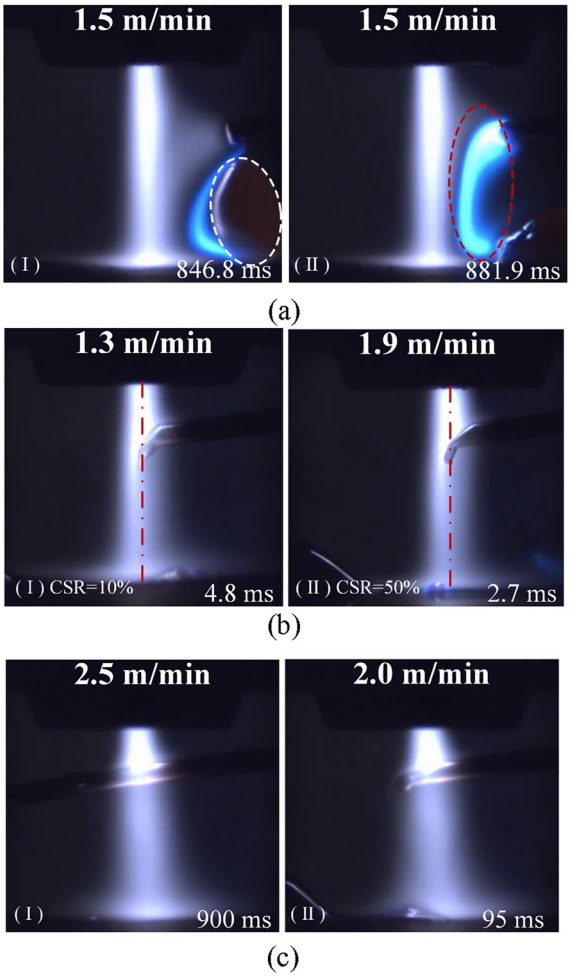

Figure 3 Schematic diagram of melting ability evaluation: (**a**) Minimum wire feeding speed, (**b**) Middle wire feeding speed, (**c**) Maximum wire feeding speed

of the wire in the arc axial direction is the distance between the filler wire and PAW torch (wire-torch distance (DWT)) (as shown in Figure 4). On the premise of the total current 100 A, the effects of a DWT of 2 mm, 3 mm, 4 mm, 5 mm and 6 mm on the melting ability with a traditional plasma arc and the effects of a DWT of 2 mm, 3 mm, and 4 mm on the melting ability under different CSRs were investigated.

The melting amount (M) is calculated based on Eq. (4):

$$M = \rho V = \rho \pi R^2 v, \tag{4}$$

where ρ is the density of wire (7.8×10^3 kg/m^3), R is the radius of wire, v is the wire melting speed (equal to wire feeding speed).

During all the experiments, an ER 70s-6 wire with a diameter of 1.2 mm was set as the filler wire, and the steel plate with a thickness of 3 mm was set as the workpiece.

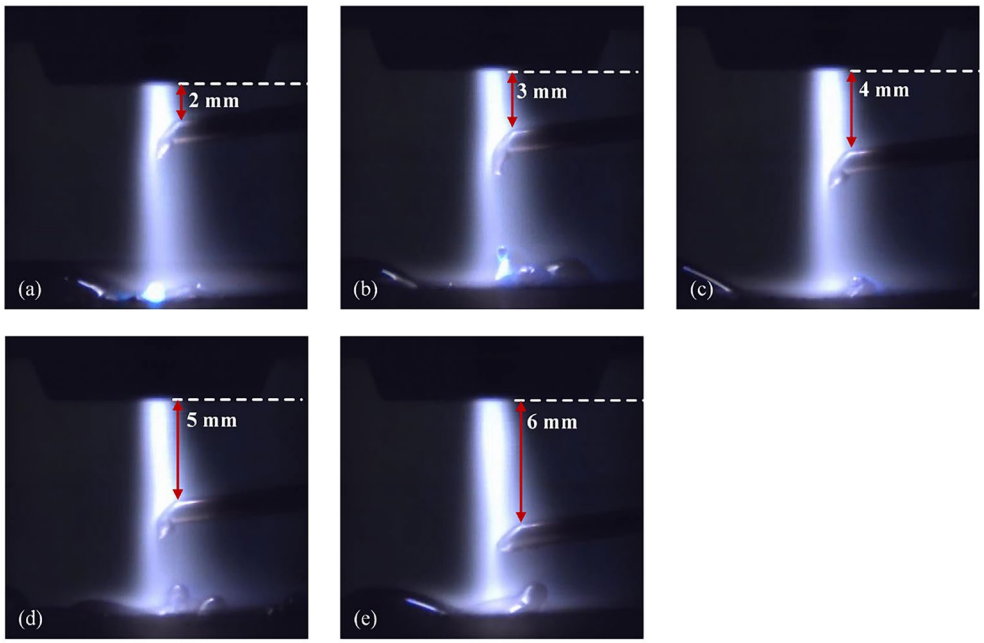

Figure 4 Schematic diagram for the position of wire in the arc axial direction

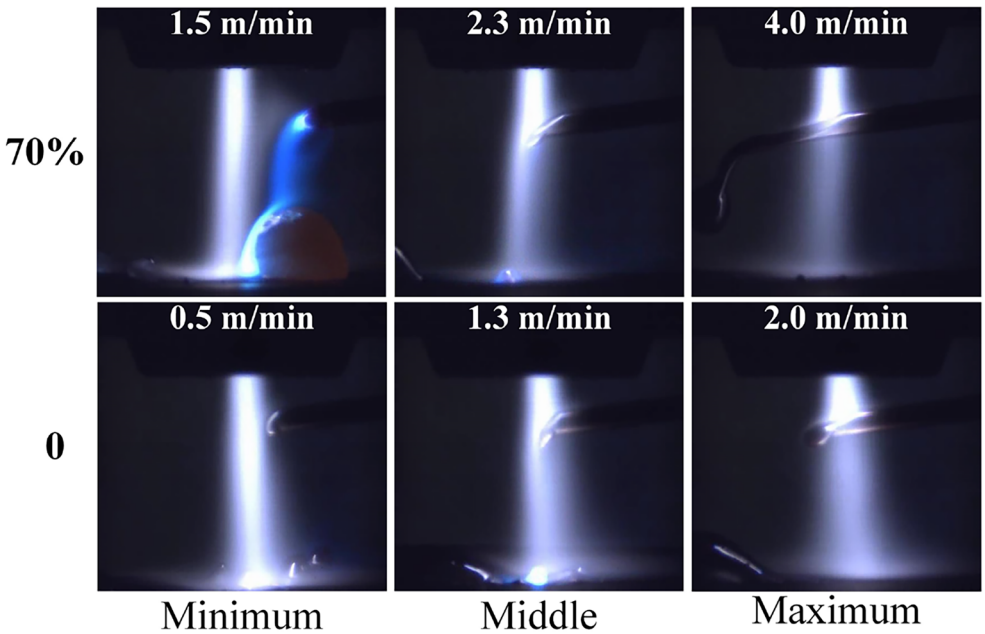

Figure 5 Typical arc images under different current separated ratios (DWT=2 mm)

The shielding gas and plasma gas were both 99.99% Ar, the shielding gas flow rate was 10.0 L/min, and the plasma gas flow rate was 3.0 L/min. The PAW torch had a 3 mm orifice diameter, a 4.8 mm tungsten electrode diameter and a 4 mm tungsten electrode setback. The distance from the torch end to workpiece was set as 10 mm.

3 Experimental Results

3.1 Control Ability of Wire Melting in Twin-Body Plasma Arc

When the total current is 100 A and the current separation ratio gradually increases from 0% to 10%, 30%, 50% and 70%, the typical arc images are shown in Figure 5. The wire melting amounts under different current separation ratios were calculated and the results are shown in Figure 6. In this figure, each vertical line represents a set of current separation ratios. "Min." means the minimum melting amount, "Mid." means the middle melting amount, and "Max." means the maximum melting amount. The length of the vertical line represents the melting mass range. The length of the blue line, which is the difference between "Mid." and "Min.", is defined as the first melting mass range, and the length of the red line, which is the difference between "Max." and "Mid.", is defined as the second melting mass range.

As shown in Figure 6, when the current separation ratio is 0 (the wire current is 0 A), the minimum melting amount is approximately 0.26 kg/h, the middle melting amount is approximately 0.69 kg/h, the maximum melting amount is approximately 1.06 kg/h, and the melting mass range is approximately 0.79 kg/h. When the current separation ratio increases to 10% (the wire current is 10 A), the minimum and middle melting amount remain unchanged, the maximum melting amount increases to approximately 0.26 kg/h, and the melting mass range increases to approximately 1.06 kg/h. When the current separation ratio increases to 30%, the minimum, middle and maximum melting amount all increase, and the melting mass range is approximately 1.32 kg/h. As the current separation ratio continues to increase, the minimum, middle and maximum melting amount all increase significantly, even showing a linear increasing trend. When the current separation ratio increases to 70%, the minimum melting amount increases by approximately 200% to approximately 0.79 kg/h, the middle melting amount increases by approximately 77% to approximately 1.22 kg/h, the maximum melting amount increases by approximately 100% to approximately 2.12 kg/h, and the melting mass range increases by approximately 66% to approximately 1.32 kg/h. With the increase in the current separation

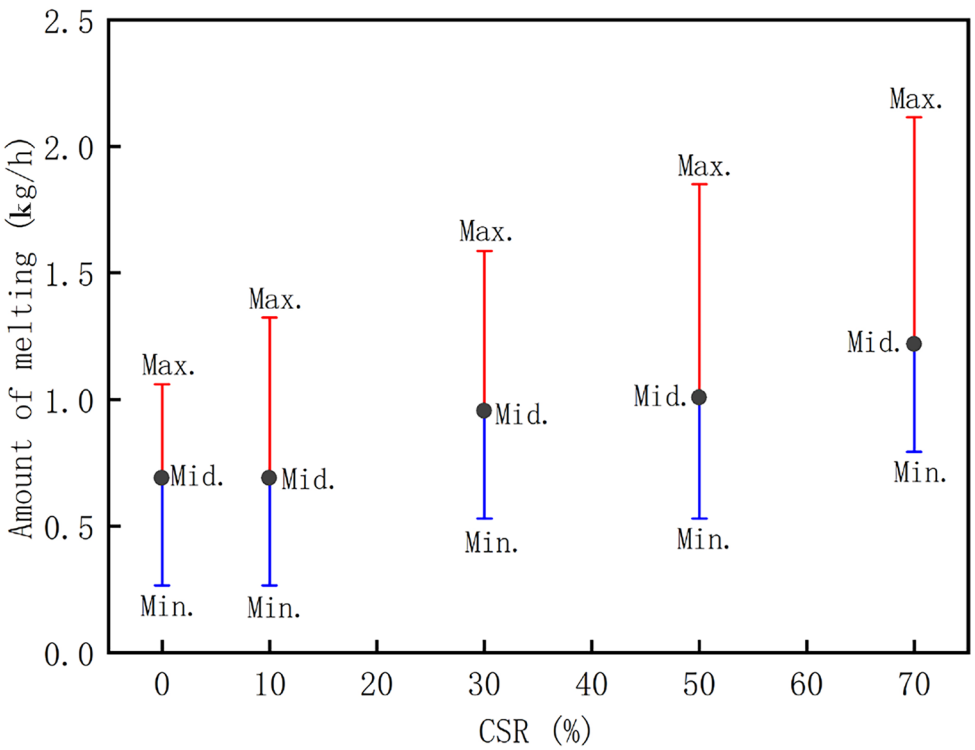

Figure 6 Wire melting amount under different current separated ratios (DWT =2 mm)

ratio, the first melting mass range remains approximately 0.42 kg/h, and the second melting mass range increases from 0.37 kg/h to 0.9 kg/h. In summary, on the premise that the total current remains unchanged, as the current separation ratio increases, the minimum and middle melting amount increase at approximately the same speed, and the first melting mass range remains unchanged; the maximum melting amount increases at twice the speed of the increase in the middle melting amount, and the second melting mass range expands.

3.2 Effect of Wire Current/Main Current on the Wire Melting Increment

In this part, the wire feeding speed was fixed and the wire melting position was changed with the wire current/main current increasing to qualitatively study the effect of the wire current/main current on the wire melting increment control ability. The wire feeding speed was fixed at 3.0 m/min, and typical arc images are shown in Figure 7. Figure 7(a) shows the typical arc images when the main current remains at 50 A and the wire current increases from 30 A to 100 A at an interval of 10 A. The melting state of the wire changes from almost no melting (wire current is 30 A) to melting (wire current is 40 A) to melting at nearly the center of the arc when the wire

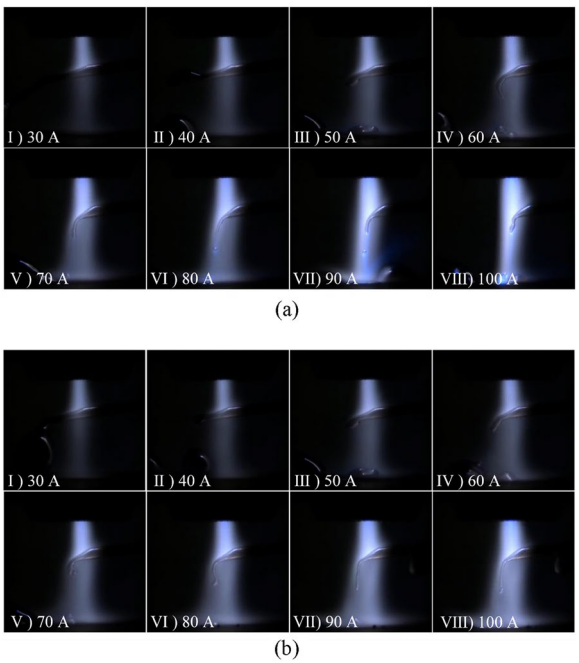

Figure 7 Typical arc images under different currents: (**a**) Wire current increases from 30 A to 100 A while the main current remains constant, (**b**) Main current increases from 30A to 100A while the wire current remains constant

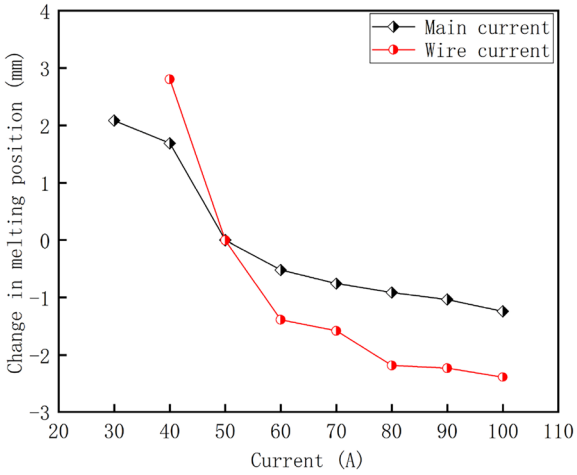

Figure 8 Relationship between the changes in melting position and currents

current increases from 30 A to 100 A. The wire melting position clearly shifts from left to right. Figure 7(b) shows the typical arc images when the wire current remains at 50 A and the main current increases from 30 A to 100 A at an interval of 10 A. When the main current increases from 30 A to 100 A, the wire is always melting, and the wire melting position also shifts from left to right, but the wire melting position remains near the left edge of the arc.

To clearly understand the change in the wire melting position, the amount of movement in the wire melting position under different currents was measured based on the wire melting position, in which the wire current and main current are both 50 A (the reference position). The relationship between the amount of movement in the wire melting position and the wire current or main current is shown in Figure 8. Because the wire is not melting when the wire current is 30 A and the main current is 50 A, the amount of movement in the wire melting position under a wire current of 30 A is not shown in Figure 8. In Figure 8, a positive value means that the wire melting position is to the left of the reference position, while a negative value means that the wire melting position is to the right of the reference position.

As shown in Figure 8, the amount of movement in the wire melting position caused by the change in main current is significantly smaller than that caused by the change in the wire current when the main current and wire current are at the same current level. The amount of movement in the wire melting position caused by the main current is approximately 1.6 mm when the main current is 40 A, and that caused by the wire current is approximately 2.8 mm when the wire current is 40 A. The range of movement in the wire melting position caused

by the main current is obviously smaller than that caused by the wire current. The range of movement in the wire melting position is approximately from 2.1 mm to −1.2 mm when the main current increases from 30 A to 100 A. The range of movement in the wire melting position changes from ∞ to approximately −2.3 mm when the wire current increases from 30 A to 100 A. Relatively speaking, the amount of movement in the wire melting position is more susceptible to the wire current than to the main current. This indicates that the wire melting increment is more susceptible to the wire current, and the effect of the wire current is significantly greater than that of the main current.

Then the wire melting position was fixed in the middle of the arc, and the middle wire feeding speed was changed as the wire or main current was increased. The effect of the wire current/main current on the wire melting increment control ability was studied quantitatively. The calculated middle melting amount is shown in Figure 9. The black line means that the middle melting amount increases as the wire current increases from 30 A to 100 A, while the main current remains at 50 A. The red line means that the middle melting amount increases as the main current increases from 30 A to 100 A, while the wire current remains at 50 A. The melting amount in Figure 9 exhibits a rapid and nearly linear increase and increases approximately from 0.79 kg/h to 1.59 kg/h when the wire current increases from 30 A to 90 A. The average increment of the melting amount is approximately 0.013 kg/h per A as the wire current increases. When the main current increases from 30 A to 90 A, the melting amount shows a slow and nearly linear increase and increases approximately from 0.95 kg/h to 1.16 kg/h. The average increment of the melting amount is approximately 0.0035 kg/h per A as the main current increases. Relatively speaking, the wire melting increment with the increase of the wire current is significantly greater than that with the increase of the main current. The average wire melting increment with the increase of the wire current is approximately 3.7 times that with the increase of the main current.

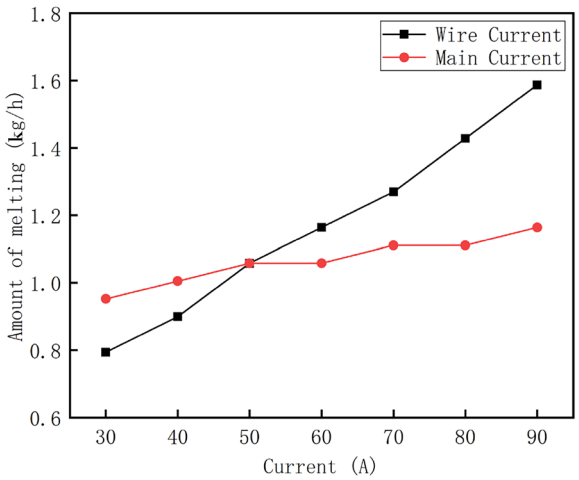

Figure 9 Melting ability under different currents

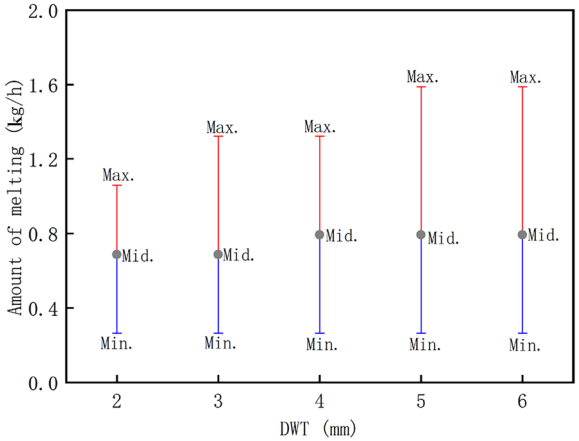

Figure 10 Melting ability under different wire-torch distances (CSR=0)

3.3 Effect of the Position of the Wire in the Arc Axial Direction on Wire Melting Amount

When the total current is 100 A and the current separation ratio is 0, the wire melting amounts under different wire-torch distances (from 2 mm to 6 mm) were calculated and are shown in Figure 10. As shown in Figure 10, the minimum melting amount is basically maintained at 0.26 kg/h as the wire-torch distance increases from 2 mm to 6 mm; the middle melting amount increases approximately from 0.69 kg/h to 0.79

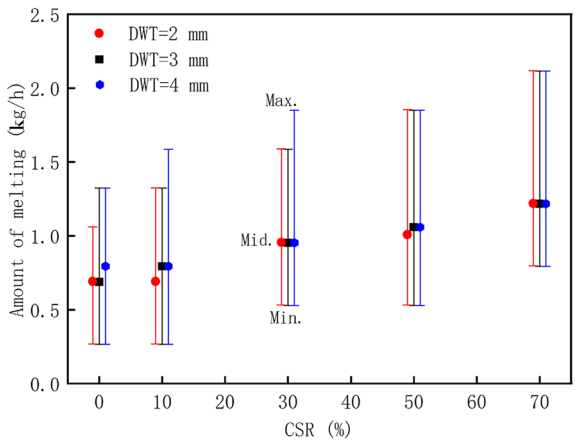

Figure 11 Comparison of the melting ability under different current separated ratios

kg/h as the wire-torch distance increases from 2 mm to 4 mm and then remains constant as the wire-torch distance continues to increase; the maximum melting amount increases approximately from 1.06 kg/h to 1.59 kg/h as the wire-torch distance increases from 2 mm to 5 mm and then remains constant as the wire-torch distance continues to increase.

Figure 11 is the line graph showing the melting amount of wire when the current separation ratio increases from 0 to 70% and the wire-torch distance increases from 2 mm to 4 mm. As shown in Figure 11, when the current separation ratio increases from 0% to 70%, the minimum melting amount remains constant at approximately 0.26 kg/h as the wire-torch distance increases from 2 mm to 4 mm. For the middle melting amount, when the current separation ratio is less than or equal to 10%, it increases by approximately 0.1 kg/h as the wire-torch distance increases from 2 mm to 4 mm. When the current separation ratio is greater than 10%, the amount of middle melting remains unchanged with the increasing wire-torch distance. For the maximum melting amount, when the current separation ratio is less than or equal to 30%, it increases by approximately 0.26 kg/h as the wire-torch distance increases from 2 mm to 4 mm. When the current separation ratio is greater than 30%, the maximum melting amount remains unchanged with the increasing wire-torch distance.

In summary, the minimum melting amount is not affected by the wire-torch distance. There is a threshold current separation ratio at which the effect of the wire-torch distance on the middle and maximum melting amount diminishes. When the current separation ratio is more than the threshold value, the middle and maximum melting amount remain constant as the wire-torch distance increases.

4 Analysis and Discussion

When the current separation ratio is 0, the total power acting on the wire corresponds to the plasma arc power. When the current separation ratio is greater than 0, the total power acting on the wire is composed of the plasma arc power and anode effect power. For the first melting mass range, the wire feeding speed is changed between 0.5 m/min and 2.3 m/min with the increase in the current separation ratio and is relatively small. The effect of wire feeding speed on the plasma arc power can be ignored, and the anode effect power is the only variable causing an increase in the middle and minimum melting amount. Therefore, the middle and minimum melting amount increase approximately synchronously with the increase in the current separation ratio, and the corresponding range remains basically unchanged. For the second melting mass range, the maximum wire feeding speed changes between 2.0 m/min and 4.0 m/min with the increase in the current separation ratio and is relatively large. The plasma arc power increases with the increasing wire feeding speed, and the plasma arc power and anode effect power are the two factors causing the increase in the maximum melting amount. Therefore, the growth rate of the maximum melting amount is twice that of the middle melting amount, and this range expands with the increase in the current separation ratio.

When the wire current remains unchanged and the main current increases, the anode effect power remains unchanged, and the plasma arc energy increases. According to Eq. (1), the plasma arc power acting on the wire increases. The plasma arc power is the only variable causing an increase in the total power acting on the wire and wire melting amount. When the main current remains unchanged and the wire current gradually increases, the anode effect power acting on the wire and the plasma arc power acting on the wire both increase with the increasing wire current. The plasma arc power and the anode effect power are the two factors causing an increase in the total power acting on the wire and wire melting amount. Therefore, the average wire melting increment with the increase of the wire current is approximately 3.7 times that with the increase of the main current increase. The average wire melting increment caused by the anode effect power is approximately 2.7 times that caused by the plasma arc power. The wire melting increment is mainly controlled by the change in anode effect power, and the plasma arc power is the second-most affected factor. The average wire melting increment is most significantly affected by the anode effect energy, and the plasma arc power is the second-most affected factor.

The radius of the plasma arc increases with the increasing wire-torch distance, and l increases. According to Eq. (1), the plasma arc power acting on the wire increases. For the minimum melting amount, it corresponds to the right edge of the arc, and the plasma arc power basically remains unchanged because the change in the wire-torch distance has little influence on the environment of the arc edge. The total power acting on the wire remains unchanged, and the minimum melting amount remains unchanged with the increasing wire-torch distance. For the middle melting amount, when the current separation ratio $\leq$10%, the anode effect power acting on the wire is relatively small (less than 50% of the increment for total power acting on the wire (as the current separation ratio increases from 0 to 70%)), the total power acting on the wire increases with the increase in the wire-torch distance, and the melting amount increases; when the current separation ratio >10%, the anode effect power is relatively great (more

than 50% of the increment for total power acting on the wire), the increment of plasma arc power caused by the increase in the wire-torch distance can be ignored, the total power acting on the wire remains constant with the increasing wire-torch distance, and the melting amount remains constant. For the maximum melting amount, when the current separation ratio ≤30%, the anode effect power acting on the wire is relatively small, and the melting amount increases with the increasing wire-torch distance; when the current separation ratio >30%, the anode effect power is relatively large, and the melting amount remains constant with the increasing wire-torch distance. Therefore, when the current separation ratio is less than the threshold value in the twin-body PA, the maximum melting amount and the middle melting amount can be adjusted by adjusting the wire-torch distance. When the current separation ratio is greater than the threshold, the wire-torch distance can be set to any value suitable for process stability.

5 Conclusions

The wire melting control ability of the twin-body plasma arc is studied by adjusting the current separation ratio (wire current), the wire current/main current and the wire-torch distance. The following conclusions can be drawn from this study:

(1) Under the premise that the total current remains unchanged (100 A), as the current separation ratio increases, the increase in plasma arc power caused by the increase in the wire feeding speed in the first melting mass range can be ignored. The middle and minimum melting amounts increase approximately synchronously under the effect of the anode effect power, and the first melting mass range remains constant. The plasma arc power increases with the increase in maximum wire feeding speed, the maximum melting amount increases twice as fast as the middle melting amount increase rate, and the second melting mass range expands.

(2) When the wire current increases, the anode effect power and the plasma arc power are the factors causing the increase in the wire melting amount; however, when the main current increases, the plasma arc power is the only factor causing the increase in the wire melting amount. The average wire melting increment with the increase of the wire current is approximately 3.7 times that with the increase of the main current. The average wire melting increment caused by the anode effect power is approximately 2.7 times that caused by the plasma arc power.

(3) The effect of the wire-torch distance on the melting amount can be divided into two parts: The minimum melting amount is not affected by the wire-torch distance under any current separation ratio, and the effect of the wire-torch distance on the middle and maximum melting amounts is determined by the threshold value of the current separation ratio. When the current separation ratio is greater than the threshold value, the anode effect power is greater, the increase in plasma arc power caused by the increase in the wire-torch distance can be ignored, and the middle and maximum melting amounts remain constant.

Acknowledgements
Not applicable.

Authors' Information
Ruiying Zhang born in 1987, is currently a lecturer at *School of Mechanical Engineering, Beijing Institute of Petrochemical Technology, China*. She received her doctoral degree from *Beijing University of Technology, China*, in 2018. Her research interests include welding arc physics and wire arc additive manufacturing.
Fan Jiang born in 1987, is currently a professor at *Faculty of Materials and Manufacturing, Beijing University of Technology, China*. He received his doctoral degree from *Beijing University of Technology, China*, in 2014. His research interests include welding arc physics, plasma arc welding and wire arc additive manufacturing.
Long Xue born in 1966, is currently a professor at *School of Mechanical Engineering, Beijing Institute of Petrochemical Technology, China*. He received his doctoral degree from *China University of Petroleum (Beijing), China*, in 2014. His research interests include special robot system and medical robot system.

Authors' Contributions
RZ designed and performed the experiments, analyzed data and wrote the manuscript; FJ developed the idea and revised the manuscript; LX assisted with manuscript revision. All authors read and approved the final manuscript.

Funding
Supported by Youth Program of National Natural Science Foundation of China (Grant No. 51905008), Beijing Postdoctoral Research Foundation of China (Grant No. 2021-zz-064), Shandong Provincial Major Science and Technology Innovation Project of China (Grant No. 2020JMRH0504), Jinan Innovation Team Project of China (Grant No. 2021GXRC066) and Quancheng Scholars Construction Project of China (Grant No. D03032).

Data availability
All data generated or analyzed during this study are included in this published article.

Declarations

Competing Interests
The authors declare no competing financial interests.

Received: 23 February 2022 Revised: 17 January 2024 Accepted: 23 February 2024
Published online: 21 March 2024

References

[1] K S Derekar. A review of wire arc additive manufacturing and advances in wire arc additive manufacturing of aluminium. *Materials Science and Technology (London)*, 2018, 34: 895–916.

[2] J Norrish, J Polden, I Richardson. A review of wire arc additive manufacturing: Development, principles, process physics, implementation and current status. *Journal of physics D: Applied Physics*, 2021, 54(47): 473001.

[3] D T Sarathchandra, S Kanmani Subbu, N Venkaiah. Functionally graded materials and processing techniques: An art of review. *Materials Today: Proceedings*, 2018, 5: 21328–21334.

[4] F Martinaa, J Mehnenb, S W Williamsa, et al. Investigation of the benefits of plasma deposition for the additive layer manufacture of Ti-6Al-4V. *Journal of Materials Processing Technology*, 2012, 212: 1377-1386.

[5] B Dong, X Y Cai, S B Lin, et al. Microstructures and mechanical properties of wire arc additive manufactured 5183-Al: Influences of deposition dimensions. *CIRP Journal of Manufacturing Science and Technology*, 2021, 35: 744-752.

[6] X Y Chen, J Han, J Wang, et al. A functionally graded material from TC4 to 316L stainless steel fabricated by double-wire + arc additive manufacturing. *Materials Letters*, 2021, 300: 130141.

[7] H J Wang, W H Jiang, J H Ouyang, et al. Rapid prototyping of 4043 Al-alloy parts by VP-GTAW. *Journal of Materials Processing Technology*, 2004, 148(1): 93-102.

[8] B Q Cong, J L Ding, S Williams. Effect of arc mode in cold metal transfer process on porosity of additively manufactured Al-6.3%Cu alloy. *The International Journal of Advanced Manufacturing Technology*, 2015, 76: 1593–1606.

[9] B Q Cong, X Y Cai, Z W Qi, et al. The effects of ultrasonic frequency pulsed arc on wire + arc additively manufactured high strength aluminum alloys. *Additive Manufacturing*, 2022, 51(3): 102617.

[10] L W Wang, T Wu, A P Liu, et al. Effect of Al–5Ti–1B grain refiner on microstructure and properties of arc-additive-manufactured Al–Mg alloy. *Vacuum*, 2022, 200: 111012.

[11] K F Ayarkwa, S W Williams, J Ding. Assessing the effect of TIG alternating current time cycle on aluminum wire + arc additive manufacture. *Addit. Manuf.*, 2017, 18: 186-193.

[12] P Kazanas, P Deherkar, P Almeida, et al. Fabrication of geometrical features using wire and arc additive manufacture. *Proceedings of the Institution of Mechanical Engineers, Part B: Journal of Engineering Manufacture*, 2012, 226: 1042-1051.

[13] C Wang, W Suder, J L Ding, et al. The effect of wire size on high deposition rate wire and plasma arc additive manufacture of Ti-6Al-4V. *Journal of Materials Processing Technology*, 2021, 288: 116842.

[14] L Wang, Y L Zhang, X M Hua, et al. Twin-wire plasma arc additive manufacturing of the Ti–45Al titanium aluminide: Processing, microstructures and mechanical properties. *Intermetallics*, 2021, 136: 107277.

[15] Y M Zhang, M Jiang, W Lu. Double-electrodes improve GMAW heat input control. *Welding Journal*, 2004, 83(11): 39-41.

[16] J S Chen, Y Lu, X R Li, et al. Gas Tungsten arc welding using an arcing wire. *Welding Journal*, 2012, 91(10): 261-269.

[17] J K Huang, Z C Guan, S R Yu, et al. Simulation and control of metal droplet transfer in bypass coupling wire arc additive manufacturing. *International Journal of Advanced Manufacturing Technology*, 2021, 115(1-2): 383-395.

[18] R Y Zhang, F Jiang, S J Chen, et al. Influence of bypass power mode on electrical properties and droplet transition of arcing-wire PAW. *Transactions of the China Welding Institution*, 2017, 38 (2): 41-46. (in Chinese)

[19] J K Huang, M H Yang, S R Yu, et al. Study on the dynamic behavior of molten pool during the stationary pileup of the double-electrode micro plasma arc welding. *Journal of Mechanical Engineering*, 2018, 54(2): 70-76.

[20] S R Yu, N D Cheng, J K Huang, et al. Relationship between thermal process and microstructure during additive manufacturing of double-electrode gas metal arc welding. *Transactions of the China Welding Institution*, 2019, 40(8): 1–6. (in Chinese)

[21] Y G Miao, C H Yin, C Wei, et al. An investigation on droplet transfer for bypass-current wire-heating PAW. *Journal of Manufacturing Processes*, 2021, 65: 355-363.

[22] R Y Zhang, F Jiang, S J Chen. Droplet transfer behaviour in twin-body plasma arc welding. *Journal of Manufacturing Processes*, 2019, 41: 330-336.

[23] R Y Zhang, F Jiang, S J Chen. Power transferred to the filler wire in twin-body plasma arc welding. *Journal of Manufacturing Processes*, 2021, 62: 566-576.